Pergamon

Bioorganic & Medicinal Chemistry 7 (1999) 2737–2748

BIOORGANIC & MEDICINAL CHEMISTRY

Molecular Dynamics of NPY Y_1 Receptor Activation

I. Sylte,[a,*] C. R. Andrianjara,[b] A. Calvet,[b] Y. Pascal[b] and S. G. Dahl[a]

[a]*Department of Pharmacology, Faculty of Medicine, University of Tromsø, -9037 Tromsø, Norway*
[b]*Institut de Recherche Jouveinal/Parke-Davies, 3-9, rue de la Loge, 94265 Fresnes Cedex, France*

Received 9 March 1999; accepted 29 June 1999

Abstract—A three-dimensional model of the human neuropeptide Y(NPY)Y_1 receptor (hY_1) was constructed, energy refined and used to simulate molecular receptor interactions of the peptide ligands NPY, [L31, P34]NPY, peptide YY (PYY) and pancreatic polypeptide (PP), and of the nonpeptide antagonist *R*-N^2-(diphenylacetyl)-*N*-(4-hydroxyphenyl)methyl-argininamide (BIBP3226) and its *S*-enantiomer BIBP3435. The best complementarity in charges between the receptor and the peptides, and the best structural accordance with experimental studies, was obtained with amino acid 1–4 of the peptides interacting with Asp194, Asp200, Gln201, Phe202 and Trp288 in the receptor. Arg33 and Arg35 of the peptides formed salt bridges with Asp104 and Asp287, respectively, while Tyr36 interacted in a binding pocket formed by Phe41, Thr42, Tyr100, Asn297, His298 and Phe302. Calculated electrostatic potentials around NPY and hY_1 molecules indicated that ligand binding is initiated by electrostatic interactions between a highly positive region in the N- and C-terminal parts of the peptides, and a negative region in the extracellular receptor domains. Molecular dynamics simulations of NPY and BIBP3226 interactions with the receptor indicated rigid body motions of TMH5 and TMH6 upon NPY binding as mechanisms of receptor activation, and that BIBP3226 may act as an antagonist by constraining these motions.

Introduction

Neuropeptide Y (NPY) is involved in several physiological processes including anxiolytic mechanisms, central endocrine secretion, regulation of food intake and control of gastrointestinal and cardiovascular functions.[1] NPY belongs to the pancreatic polypeptide family (PP-family) of homologous peptides which also includes the gut peptide YY (PYY) and the pancreatic polypeptide (PP). All these have a primary structure of 36 amino acids and an amidated C-terminal. Apparently, all these peptides adopt a common hairpin-like tertiary structure (PP-fold) as observed in the X-ray structure of avian PP.[2] The X-ray structure of avian PP has an N-terminal polyproline type II helix (residues 1–8), a turn (residues 9–14), an amphipatic helix (residues 15–32) arranged antiparallel to the polyproline helix, and a flexible C-terminal part. A similar overall structure was observed in the solution NMR structure of bovine PP[3] and human NPY,[4] although NPY seems to be more flexible than PP in solution. However, a dimeric NMR structure of NPY in solution suggests that the C-terminal helical structure extends to residue 36.[5]

Receptor binding studies using NPY, PYY, PP and NPY analogues have identified six receptor subtypes distinguished by their affinity for the PP-family of peptides. These receptors are designated Y_1, Y_2, Y_3, Y_4, Y_5 and PYY preferring receptor.[1] The human Y_1 receptor (hY_1),[6,7] rat Y_1 receptor (rY_1),[8] human Y_2 receptor,[9] human Y_4 receptor,[10,11] and the mouse[12] and rat[13] Y_5 receptors have been cloned, and all belong to the superfamily of guanine nucleotide binding regulatory protein (G-protein) coupled receptors (GPCRs). The GPCRs have seven transmembrane α-helices (TMHs) in analogy with bacteriorhodopsin[14] and rhodopsin.[15] Y_1 is the structurally best characterized NPY receptor. Site directed mutagenesis studies of the hY_1[16–18] and the rY_1[19,20] have shown that NPY interacts with amino acid residues in the extracellular (EC) loops and in the EC ends of the TMHs.

We have constructed a three-dimensional model of the hY_1,[†] with the TMHs packed in an arrangement derived from the projection map of bovine rhodopsin.[21] The

Key words: NPY Y_1-receptor; ligand interactions; molecular dynamics; receptor activation.
* Corresponding author. Tel.: +47-77-64-47-05; fax: +47-77-64-53-10; e-mail: sylte@fagmed.uit.no
† The coordinates are available from the authors upon request (e-mail: sylte@fagmed.uit.no)

0968-0896/99/$ - see front matter
PII: S0968-0896(99)00229-1

intracellular (IC) and EC regions were modeled using secondary structure prediction, manual adjustments according to the results of site directed mutagenesis studies of the rY_1 and hY_1,[16–20] and simulated annealing molecular dynamics simulations. The model was used to study the receptor interactions of NPY, [L31, P34]NPY, PYY and PP, and of the small molecule antagonists *R*-*N*^{2}-(diphenylacetyl)-*N*-(4-hydroxyphenyl)-methyl-argininamide (BIBP3226) and its *S*-enantiomer, BIBP3435. Receptor binding energies and molecular electrostatic potentials were calculated, and from all this a molecular mechanism of Y_1 receptor activation is proposed.

Results

Receptor structure

The TMHs of the receptor were modeled according a proposed common packing of the TMHs in GPCRs,[21] with TMH1 and TMH4 most exposed and TMH3 and TMH7 least exposed to the lipid membrane. Tyr100, which has been identified as a key residue for binding of NPY,[17] was located at the EC end of TMH2 (Fig. 1), while Tyr211 which has been identified as important for binding of BIBP3226,[18] was located at the EC end of TMH5 (Fig. 1). Asp287, which has been identified as a key residue for binding of both NPY and BIBP3226,[18] was located at the EC end of TMH6 (Fig. 1). The side chains of Tyr100, Tyr211 and Asp287 were all pointing into the central pore created by the TMHs.

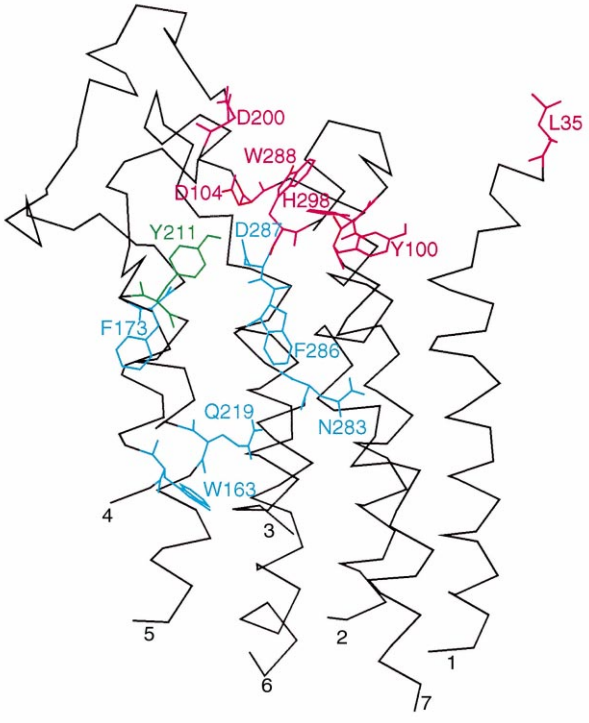

Figure 1. C_α-atom carbon trace of the TMHs and the EC-parts (amino acids 1–34 are deleted) of the receptor model. The TMHs are indicated by numbers. Amino acid side chains shown by site directed mutagenesis studies of the hY_1 or rY_1 receptor to be important for ligand binding are indicated. Red: side chains of importance for binding NPY. Yellow: side chain important for binding BIBP3226. Blue:

Trp163, which is important for binding both of NPY and BIBP3226[18] to the Y_1 receptor, was located two helical turns from the IC end of TMH4 (Fig. 1). This could indicate that the function of Trp163 is to maintain a proper receptor structure for ligand binding, rather than a direct ligand interaction. In the average structure of ligand–receptor complexes observed between 255 and 355 ps of simulation, Trp163 was packed against amino acids in TMH3, and also interacted with Arg138 at the EC end of TMH3 and with Asn151 and Trp148 in IC 2.

Phe173 in hY_1, which also is important for binding of NPY and BIBP3226,[18] was located one helical turn from the EC end of TMH4 (Fig. 1), adjacent to the highly conserved Pro174. The side chain of Phe173 was packed against the side chains of Leu214, Leu215 and Leu218 in TMH5, and against the side chain of Ser169 in TMH4.

Gln219, which also is a key residue for binding of NPY and BIBP3226 to hY_1[18] was located three helical turns from the EC end of TMH5 (Fig. 1). The side chain of Gln219 was hydrogen bonded with Ser127 in TMH3, and interacted with Trp276 in TMH6. Gln219 was shielded against direct ligand interactions by Asp287, which is important for binding of NPY and BIBP3226 to rY_1,[19] and by Trp288 which is important for binding of NPY to rY_1.[20]

Asn283, also important for binding of NPY and BIBP3226,[18] was located 1–2 helical turns from the EC end of TMH6 (Fig. 1). The side chain of Asn283 was packed against Leu304, Leu307 and Ile311 in TMH7. The side chain of Phe286, which is important for binding of NPY and BIBP3226,[18] was packed against Leu300 and Leu304 in TMH7.

Of the EC segments, the N-terminal was most distant from the putative NPY binding site. However, the region around His34-Ile40 may contribute to the binding of NPY via long-range electrostatic interactions.[19] The relatively short EC loop 1 connecting TMH2 and TMH3, had segment Glu110-Lys114 packed against EC loop 2. Asp104, a key residue for binding of NPY but not for BIBP3226,[18] was facing the central pore created by the TMHs (Fig. 1). EC loop 2 which is longer than EC loop 1, was extending toward the EC side of the model with possible key residues for NPY binding (Asp194, Asp200, Asp205) located at the surface of the loop (Fig. 1), and capable of forming ligand interactions. The structure of EC loop 2 was stabilized by strong intramolecular electrostatic interactions: Lys193 with Asp194 and Asp200, Lys195 with Asp190, Asp194 and Asp200, and Arg208 with Asp182 and Asp205. EC loop 3 formed a rather short span between TMH6 and TMH7, with Trp288 and His298 facing the central pore formed by the TMHs (Fig. 1). Trp288 and His298 have previously been identified as key residues for NPY binding.[18,20]

The molecular electrostatic potentials show that the hY_1 receptor is mainly negative in the synaptic domains and positive in the cytoplasmic domains (Fig. 2). The most positive area was outside IC loop 3 where residues Lys233, Arg237, Lys239, Arg240, Arg241, Arg252 and Arg254 together with Arg72 in IC loop 1 and His154 in IC loop 2 created an area exposed to the cytosol, with electrostatic potentials above 40 kcal/mol. The lowest electrostatic potentials were seen around Asp287 at the EC end of TMH6. The side chain of Asp287 created electrostatic potentials lower than −40 kcal/mol in the area lining the central pore of the receptor model. The molecular surfaces of NPY and PP, color coded according to the electrostatic potentials, are shown in Figure 3. A similar charge distribution was also seen for [L31, P34]NPY and PYY, and was confirmed by calculations with the GRASP program[22] (data not shown).

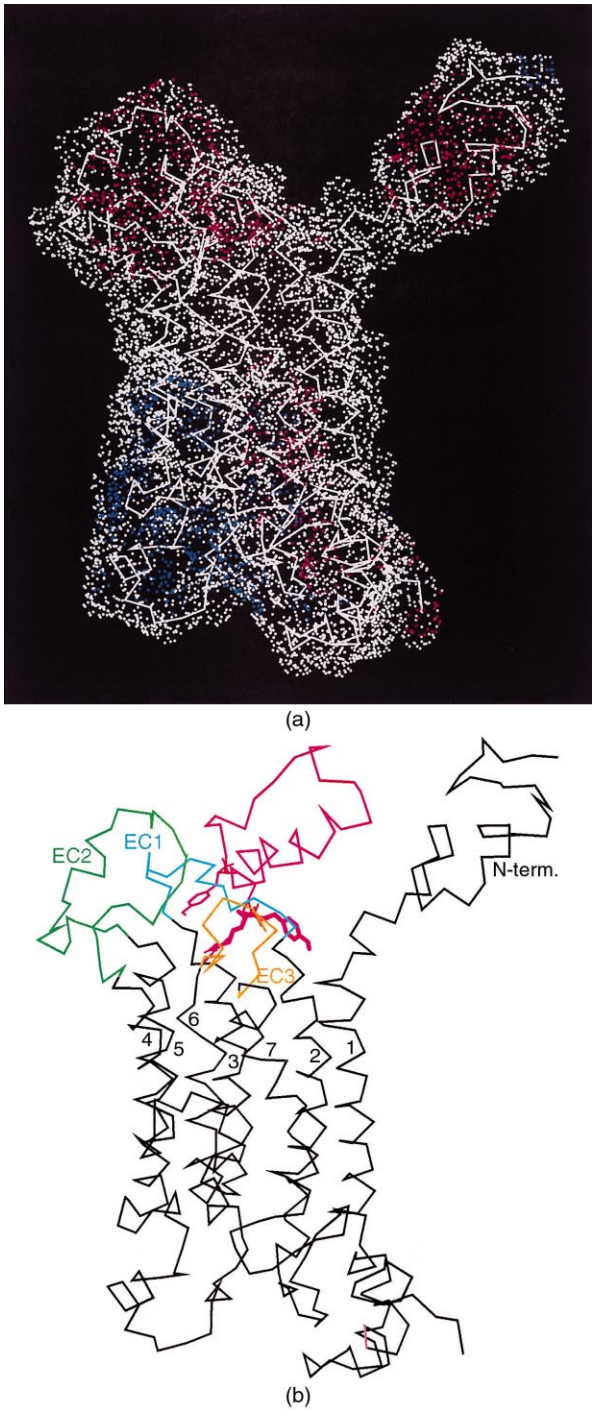

Figure 2. Above: Water accessible surface of the hY_1 receptor model color coded according to electrostatic potentials (e) 1.4 Å outside the surface: red, $e < -18$ kcal/mol; white, -18 kcal/mol $< e < 18$ kcal/mol; blue, $e > 18$ kcal/mol. The extracellular side is up in the figure with the N-terminal to the right. Below: C_α-atom carbon trace of the energy minimized average of NPY-hY_1 structures observed between 255 and 355 ps of simulation, viewed in the membrane plane. The TMHs are indicated by numbers.

Receptor—PP-family peptide interactions

The receptor docking mode of NPY that gave best complementarity in distribution of charged amino acids and best accordance with site directed mutagenesis studies, was with Tyr1 of NPY in the direction of Trp288 in EC loop 3 (Fig. 4). Arg33 in NPY was orientated towards Asp104 in EC loop 1, while Arg35 was orientated towards Asp287 in TMH6. The amidated Tyr36 was localized in a pocket consisting of His298 in EC loop 3, Tyr100 in EC loop 1 and Phe42 in TMH1.

In the energy minimized average structure from 255 to 355 ps of simulation, several more amino acids of NPY had van der Waals contacts with the receptor model than after the initial docking (Figs 2 and 4). However, the interaction was maintained between residues in the hY_1 receptor identified experimentally as key residues for NPY binding (Tyr100, Asp104, Asp287, Trp288, His298), and key residues in NPY (Tyr1, Arg33, Arg35, Tyr36-NH_2) for binding to the Y_1 receptor[23–26] (Fig. 4). In the energy minimized average structure from 255 to 355 ps of simulation, Tyr1 in NPY had aromatic stacking interactions with Trp288 in EC loop 3, while the hydroxyl group of Tyr1 interacted in a pocket formed by Gln201, Phe202 in EC loop 2 and Ile293 in EC loop 3. Lys4 in NPY interacted strongest with Asp194 and Asp200 in EC loop 2 (Fig. 4). Arg33 in NPY interacted strongly with Asp104 in EC loop 1, and also with Cys113 and other residues in EC loop 1, and with Cys198 in EC loop 2. The side chain of Arg35 had van der Waals contacts with Asn116 in TMH3, Asp287 in TMH6, Trp288 and His298 in EC loop 3, and Leu302 in TMH7. Phe173 was located about 7 Å from the side chain of Arg35 in NPY, and was shielded by Tyr176 at the EC end of TMH4 and Tyr211 at the EC end of TMH5 for a direct ligand interactions. The amide group of Tyr36 was hydrogen bonded with His298. The hydroxyl group of Tyr36 was hydrogen bonded with Tyr100 in TMH2 and Thr42 in TMH1, while the ring system of Tyr36 interacted with Phe41 in TMH1, Asn297 in EC loop 3 and Phe302 in TMH7 (Fig. 4).

Calculation of ligand-receptor binding energies suggested that the PP-family of peptides bind to hY_1 in the rank order PYY > [L31, P34]NPY > NPY > > PP (Table 1). These calculated ligand-receptor binding energies are in reasonably good agreement with the rank order of experimentally detected binding affinities [6] : PYY > NPY > [L31, P34]NPY > > PP. As indicated in Table 1, NPY, [L31, P34]NPY and PYY introduced greater

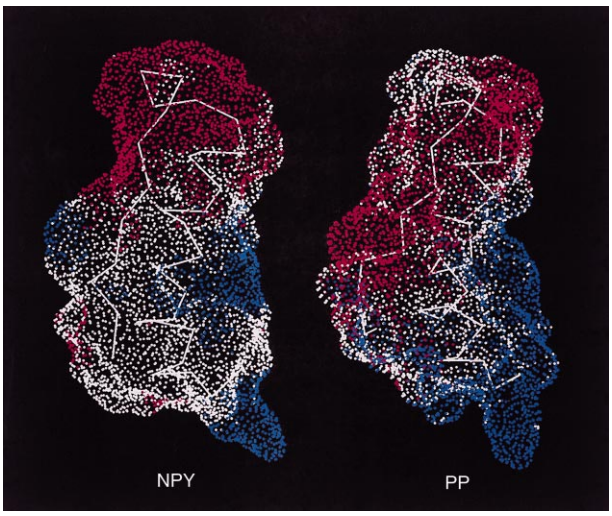

Figure 3. Water accessible surface and electrostatic potentials (e) 1.4 Å outside the surface of NPY and PP. Color coding of electrostatic potentials: red, $e < -18$ kcal/mol; white, -18 kcal/mol $< e <$ 18 kcal/mol; blue, $e > 18$ kcal/mol.

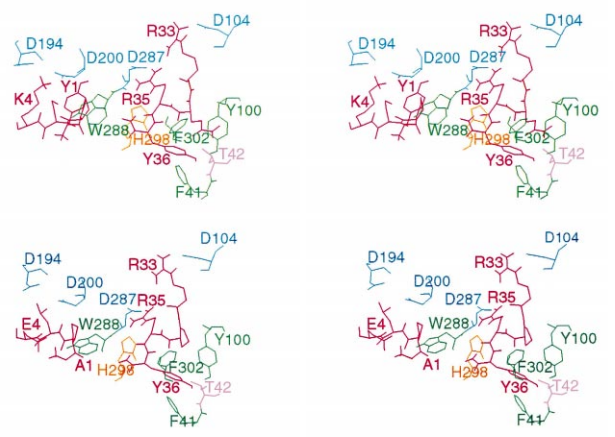

Figure 4. Above. Stereo illustration showing the binding interactions in the energy minimized average NPY-hY_1 receptor complex. The following amino acids in NPY are shown (red): Tyr1 (interacting with W288), Pro2, Ser3, Lys4 (interacting with D194 and D200), Arg33 (interacting with D104), Gln34, Arg35 (interacting with D287) and Tyr36 (interacting in the region of Y100 and F302). Below. Stereo illustration showing the binding interactions in the energy minimized PP-hY_1 receptor complex. The following amino acids in PP are shown (red): Ala1 (in the region of W288), Pro2, Leu3, Glu4 (in the region of D194 and D200), Arg33 (interacting with D104). Pro34, Arg35 (interacting with D287) and Tyr36 (interacting in the region of Y100 and F302). The complexes are viewed from the extracellular side.

structural changes in the receptor upon binding than did PP. However, these structural changes were compensated by a much higher molecular interaction energy (E_{INT}) between the peptide and the receptor for NPY, [L31,P34]NPY and PYY than for PP. The most important amino acid residues in the peptides for binding to the receptor model are shown in Table 2.

Receptor—BIBP3226 interactions

The structure of BIBP3226 is shown in Scheme 1. In the energy minimized average structure from 150 to 250 ps, the guanidinium group of BIBP3226 interacted strongest with the side chain of Asp287 in TMH6, Asn116 in TMH3 and Asn297 in EC loop 3 (Fig. 5). The hydroxyphenyl ring of BIBP3226 interacted with the main chain carbonyl group of Asp200 in EC loop 2, the side chain of Gln201 and Phe202 in EC loop 2, Tyr211 in TMH5 and Trp288 in EC loop 3. One of the phenyl rings interacted with the main chain carbonyl group of Tyr100, the side chain of Met103 EC in loop 1, Val119 in TMH3 and Phe302 in TMH7. The other phenyl ring interacted with the side chain of Met103 and the backbone atoms of His105 in EC loop 1, Phe199 in EC loop 2 and Phe302 in TMH7 (Fig. 5). Amino acids with van der Waals contact with BIBP3226 and BIBP3435 are shown in Table 3.

The calculated binding energies indicated that BIBP3226 binds much more strongly to hY_1 than did the *S*-enantiomer BIBP3435 (Table 1), because the *S*-enantiomer interacted more weakly with Asp287 (TMH6). BIBP3435 did not have the possibility of favorable interactions between its phenyl rings and the receptor, and several more amino acids in the receptor had van der Waals contacts with BIBP3226 than with BIBP3435 (Table 3).

Molecular dynamics of receptor–ligand interactions

The structure of hY_1 in complex with NPY was considered as the activated receptor structure, while the structure of hY_1 in complex with BIBP3226 was considered as the deactivated receptor structure. Table 4 indicates that the most striking structural differences in the TMHs between the activated receptor structure and the deactivated receptor structure were in TMH5 and TMH6. The R.M.S. of fluctuation (backbone atoms) relative to the energy minimized mean structure, averaged over the observed complexes between 255 and 355 ps, indicated that TMH5 and TMH6 were fluctuating more than the other TMHs during the simulation with NPY (Table 4). This may indicate that NPY introduced larger structural movements of TMH5 and TMH6 than of the other TMHs. The simulation with BIBP3226 indicated that the antagonist did not introduce larger structural movements of TMH5 and TMH6 than of other TMHs (Table 4).

Discussion

Considerable effort has been devoted to molecular modeling of GPCRs during the last years, which has proved helpful in identifying ligand binding sites and obtaining a better understanding of molecular receptor mechanisms. Based on the electron density projection map of visual rhodopsin and on site directed mutagenesis studies of GPCRs, a general arrangement of the TMHs in GPCRs has been proposed.[21] This arrangement was corroborated by the recent projection map of frog rhodopsin,[15] supporting the notion that this pro-

Table 1. Ligand–receptor binding energies[a]

Ligand	E_{INT} (kcal/mol)	E_{LD} (kcal/mol)	E_{RD} (kcal/mol)	E_B (kcal/mol)
NPY	−356.3	73.5	30.8	−252.0
[L31,P34]NPY	−363.0	76.4	22.4	−264.2
PYY	−379.3	72.1	35.9	−271.3
PP	−314.3	71.7	19.1	−223.5
BIBP3226	−102.4	27.7	3.6	−71.1
BIBP3435	−56.0	29.1	3.5	−22.4

[a] Calculated ligand–receptor binding energies (E_B) for NPY, NPY analogues, BIBP3435 and BIBP3226. E_{INT}: total interaction energy between ligand and receptor in the energy minimized complex. E_{LD}: distortion energy of the ligand upon binding. E_{RD}: distortion energy of the receptor upon binding.

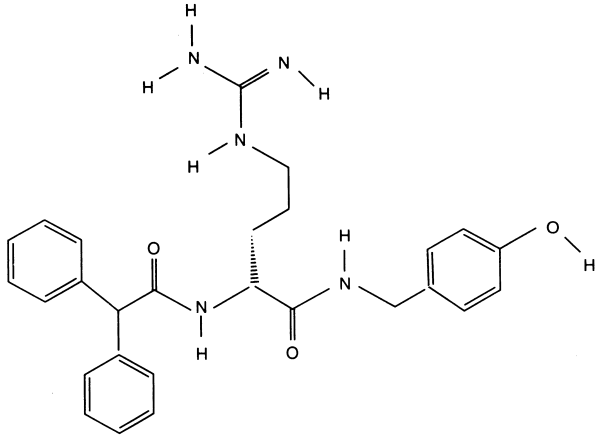

Scheme 1. Chemical structure of BIBP3226.

posed arrangement may be used to construct reliable models of TMHs of GPRCs.

The EC and IC regions are the most divergent parts of GPCRs, differing both in length and sequence, and only a few models of GPCRs have included the entire EC and IC domains. The most common approaches in modeling of the EC and IC parts have been to use secondary structure predictions combined with structure refinement by molecular mechanics calculations and molecular dynamics simulations,[27,28] using starting structures from loop databases,[29] and using results from site-directed mutagenesis studies as a guide to build the loops such that key residues may interact with ligands.[30] Site directed mutagenesis studies of the Y_1 receptor have shown that high affinity binding of NPY to the Y_1 receptor is highly dependent on acidic and aromatic residues in the EC parts.[16–20] Therefore, the EC domains have to be included in order to model the interactions between the Y_1 receptor and its ligands. The *N*-terminal was not included in a previous model of the hY_1.[30] However, recent site directed mutagenesis studies of the rY_1 receptor have indicated that the *N*-terminal is important for binding of NPY,[19] and it was, therefore, included in the present model. In the present study we have used an approach based on secondary structure predictions guided by results from previous site-directed mutagenesis studies, and simulated annealing molecular dynamics for structure refinement, to model the EC receptor domains. However, as for other GPCR models, the EC and IC parts still are the structurally most uncertain parts of the present receptor model.

Experimental support for the hY_1 model

The arrangement of TMHs in the receptor model is in accordance with interhelical interactions proposed from experimental studies. Asp86 in TMH2 forms hydrogen bonds with Asn58 in TMH1, Asn316 in TMH7 and Tyr320 in TMH7, constituting a hydrogen bonding network which constrains TMH1, TMH2 and TMH7 relative to each other. These residues are highly

Table 2. Molecular interaction energy between residues in the peptide ligands and the receptor[a]

Molecular interaction energy (kcal/mol) with the human Y_1 receptor model							
NPY		[L31, P34]NPY		PYY		PP	
Tyr1	−33.8	Tyr1	−35.0	Tyr1	−37.6	Ala1	−11.5
Pro2	−4.1	Pro2	−4.1[b]	Pro2	−2.7	Pro2	−6.0
Ser3	−1.2	Ser3	−1.1[b]	Ile3	−3.9[b]	Leu3	−6.4
Lys4	−60.9	Lys4	−61.2	Lys4	−60.0	Glu4	3.3[b]
Arg19	−2.6[b]	Arg19	−3.9[b]	Arg19	−15.1	Gln19	−0.5[b]
Ala23	−1.9[b]	Ala23	−2.0[b]	Ser23	−2.1[b]	Asp23	−4.4
Arg25	−5.1	Arg25	−4.8	Thr25	−0.2[b]	Arg25	−3.9
His26	−4.6	His26	−4.9	His26	−4.5	Arg26	−32.9
Tyr27	−15.6	Tyr27	−15.5	Tyr27	−15.5	Tyr27	−15.6
Leu30	−9.7	Leu30	−9.7	Leu30	−9.7	Met30	−12.7
Ile31	−8.3	Leu31	−8.1	Val31	−7.1	Leu31	−8.6
Thr32	−2.1	Thr32	−2.4	Thr32	−2.5	Thr32	−2.6
Arg33	−78.7	Arg33	−81.5	Arg33	−82.0	Arg33	−80.6
Gln34	−14.1	Pro34	−7.8	Gln34	−13.8	Pro34	−7.8
Arg35	−86.4	Arg35	−89.0	Arg35	−88.4	Arg35	−89.2
Tyr36	−26.6	Tyr36	−30.9	Tyr36	−31.9	Tyr36	−30.6

[a] Residues having van der Waals contact with the receptor in at least one of the receptor–peptide complexes are included in the table.
[b] Amino acids outside van der Waals contact with the receptor.

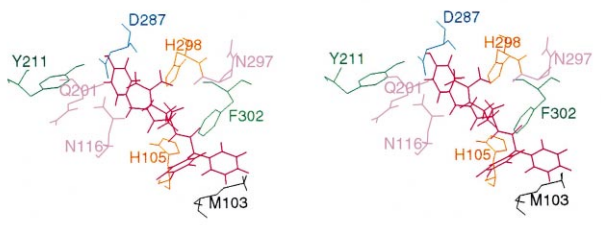

Figure 5. Stereo illustration showing the binding interactions in the energy minimized average BIBP3226-hY_1 receptor complex, viewed from the IC-side of the receptor. BIBP3226 is shown in red.

conserved among the GPCRs. A direct interaction between residues corresponding to Asp86 and Asn316 has also been proposed by site directed mutagenesis studies of the gonadotropin-releasing hormone receptor,[31] and the 5-HT_{2a} receptor.[32] Site directed mutagenesis studies of the thyrothropine-releasing hormone receptor have confirmed the existence of a direct interaction between Asn58 in TMH1 and Asp86 in TMH2.[33] In that study, it was suggested that the residue corresponding to Asp86 in TMH2 bridges the asparagine residues corresponding to Asn58 and Asn316, which is consistent with the present hY_1 model. Site directed mutagenesis studies of the rY_1 receptor have also confirmed the importance of the residue corresponding to Asp86 in hY_1 for maintaining a proper structure for NPY binding.[19] Site directed mutagenesis studies of the human β_2-receptor identified the tyrosine residue corresponding to Tyr320 in hY_1 as a critical determinant for maintaining a proper receptor conformation.[34]

Site directed mutagenesis studies of muscarinic M1/M5 receptor chimers[35] suggested that residues corresponding to Tyr47 (TMH1) and Leu303 (TMH7) in hY_1 are facing each other. In the present model, these residues are located close to each other in the helical bundle, with the possibility of direct hydrophobic contacts between their side chains.

Table 3. Molecular interaction energies (kcal/mol) between amino acids in the receptor and BIBP3226 and BIBP3435[a]

BIBP3226		BIBP3435	
Leu102	−2.2	Asn116	−4.8
Met103	−8.7	Gln201	−4.7
His105	−3.7	Asp287	−12.0
Val107	−2.6	Trp288	−5.1
Asn116	−8.0	His298	−7.5
Val119	−1.5	Leu301	−1.3
Phe199	−3.4	Phe302	−3.6
Asp200	−3.8		
Gln201	−5.6		
Phe202	−2.4		
Tyr211	−1.6		
Asp287	−38.4		
Trp288	−4.2		
Asn297	−7.8		
His298	−11.4		
Leu301	−2.1		
Phe302	−3.8		

[a] The energy minimized average complex of BIBP3226 and the receptor between 150 and 250 ps of simulation, and the energy minimized complex of BIBP3435 and the receptor are included in the table. Amino acid residues in the receptor having van der Waals contacts with ligands are included.

Based on molecular modeling and site directed mutagenesis studies of the AT_{1a} angiotensin receptor, it has been suggested that Asn111 in TMH3 of the AT_{1a} receptor is located close to Tyr292 in TMH7[36] and Asn295 in TMH7.[37] These residues correspond to Ser123 in TMH3, Met310 and Thr313 in TMH7 in hY_1. In the present model Ser123 interacted directly with Met310, while the side chains not are long enough for a direct interaction between Ser123 and Thr313.

The relative orientations of TMH1, TMH2, TMH6 and TMH7 in the present model is in accordance with studies of chimeric α_2/β_2 adrenergic receptors,[38] placing the side chain of Leu311 in TMH7 of the β_2-adrenergic receptor between TMH3 and TMH6, and Asn312 between TMH1 and TMH2. These residues correspond to Cys305 and His306 in hY_1. The side chain of Cys305 pointed towards Gln120 in TMH3, and Thr284 and Val285 in TMH6, while the side chain of His306 pointed towards Thr41 in TMH1 and Thr97 in TMH2.

The orientations of TMH2 and TMH7 relative to each other are supported by the Gly90Asp exchange in visual rhodopsin, which causes congenital night blindness. It has been demonstrated that Asp90 in TMH2 of mutated visual rhodopsin is proximal to Lys296 in TMH7.[39] These residues correspond to Cys93 in TMH2 and Met310 in TMH7 of the hY_1 receptor. In the present model these residues are located in close proximity, with a 3.5 Å distance between their sulphur atoms.

Further support for the present model is given by studies introducing an artificial Zn^{2+} binding site into the human NK_1[40,41] and rat κ-opioid[42] receptors. These studies suggest that amino acid residues corresponding to Tyr100 (TMH2) and Asn116 (TMH3), and residues corresponding to Thr212 (TMH5) and Asp287 (TMH6) of hY_1 are facing each other. The Thr212-Asp287 residue pair is located at the EC end of the TMHs, with the side chain of Thr212 pointing towards the side chain of Asp287. Tyr100 and Asn116 located at EC end of the TMHs are also facing each other. In the energy minimized average structure from 255 to 355 ps of simulation with NPY, the side chains of Tyr100 and Asn116 were both involved in binding of NPY.

All these experimental results with different GPCRs support the packing arrangement of TMH1, TMH2, TMH3, TMH5, TMH6 and TMH7 in the present hY_1 model. In order to further validate the three-dimensional structure of the model, particularly the orientation of TMH4 relative to other TMHs, further experimental studies of interhelical interactions are required.

Ligand–receptor interactions

Accounting for the flexibility of ligands represent a challenge in molecular modeling of ligand–receptor interactions, since the receptor-bound ligand may adopt a conformation with potential energy above its global

Table 4. R.M.S. differences between receptor structures after simulation with NPY and BIBP3226[a]

Receptor domain	R.M.S. difference	R.M.S. fluct. NPY	R.M.S. fluct. BIBP3226
TMH1, amino acids 40–67	1.24	0.47	0.48
TMH2, amino acids 78–100	0.32	0.35	0.44
TMH3, amino acids 115–136	0.83	0.41	0.68
TMH4, amino acids 156–176	0.96	0.58	0.61
TMH5, amino acids 210–233	1.25	0.63	0.58
TMH6, amino acids 264–287	1.39	0.75	0.58
TMH7, amino acids 301–324	0.86	0.47	0.54

[a] R.M.S. difference: The R.M.S. difference of TMHs (backbone atoms) between the energy minimized average receptor-NPY (255–355 ps) and receptor-BIBP3226 (150–250 ps) complexes. R.M.S. fluct. NPY: The R.M.S. of fluctuations (backbone atoms) relative to the energy minimized mean structure (255–355 ps of simulation), averaged over the observed coordinate sets between 255 and 355 ps of simulation with NPY. R.M.S. fluct. BIBP3226: The R.M.S. of fluctuations (backbone atoms) relative to the energy minimized mean structure (150–250 ps of simulation), averaged over the observed coordinate sets between 150 and 250 ps of simulation with BIBP3226.

energy minimum. BIBP3226 and BIBP3435 are structurally flexible molecules, and several different low-energy conformations were considered in the docking of BIBP3226 and BIBP3435 into the model. The conformations that gave the best structural fit with the receptor model had about 2 kcal/mol higher energy then the lowest-energy conformations of BIBP3226 and BIBP3435. It has been suggested that NPY has a more flexible C-terminal than PP, and that NPY may adopt a low-energy conformation slightly different form the X-ray crystal structure of avian PP.[5] The problem with structural flexibility of the ligand may partly be overcome by molecular dynamics simulations of the ligand–receptor complex, giving the receptor and ligand freedom to adopt complimentary conformations. However, the structure of the receptor-bound ligand may still be dependent on the initial structure of the ligand and the receptor. Therefore, the possibility that other ligand conformations may interact with the receptor can not be ruled out.

The present method for calculating ligand–receptor binding energies has previously given good correlations to experimentally measured binding constants for the κ-opioid receptor[43] and the 5-HT_{1a} receptor.[28] However, this method is limited by the structural accuracy of the receptor and peptide models. In aqueous solution, a driving force for binding is the increase of entropy due to the disappearance of ordered water–ligand and water–receptor contacts, which was not taken into account in the present calculations. The method does take into account the structural changes in the receptor and the ligand upon binding, and might, therefore, be expected to be better correlated to experimental binding data than the molecular interaction energy (E_{INT}) between the receptor and the ligand. Therefore, the method may be useful for comparing ligands with high structural similarity, like the PP-family peptides, since the methodological limitations should be similar for ligands with high structural similarity. However, the calculated binding energies of BIBP3226 and BIBP3435 may not be directly compared with the calculated binding energies of the PP-family peptides.

The rank order of calculated receptor binding energies of the PP-family peptides was in reasonably good agreement with experimentally measured affinities,[6] indicating a realistic orientation of the peptides at the hY_1 receptor. Further support for the binding mode of NPY and BIBP3226 is given by site directed mutagenesis studies of the Y_1 receptor,[18] which have suggested that Trp288 is important for binding of NPY but not for BIBP3226, while Tyr211 is important for binding of BIBP3226 but not for NPY. In the present model, Trp288 had aromatic π–π interactions with Tyr1 in NPY, and was only weakly involved in binding to BIBP3226, while Tyr211 was hydrogen bonded with the hydroxyphenyl group of BIBP3226, and only weakly involved in binding to NPY.

Site directed mutagenesis studies of the hY_1 receptor have indicated that the side chains of Tyr100, Asp104 and His298 are important for binding of NPY but not for BIBP3226.[18] The present simulation of NPY-Y_1 receptor interactions maintained the interactions of NPY with the side chain of these residues. During the simulations of BIBP3226-receptor interactions, Asp104 was not involved in binding of BIBP3226, while the backbone atoms of Tyr100 and His298 were involved in binding to BIBP3226 (Table 3). Site directed mutagenesis studies have shown that the side chain of His105 is not important for binding NPY or BIBP3226,[18] and the present simulation suggested that BIBP3226 interacted with the backbone atoms of His105. Binding studies with Tyr100Ala, His105Ala and His298Ala mutants, did not show any effect of these mutations on BIBP3226 binding to the hY_1 receptor. This is in accordance with the present model which proposes a direct BIBP3226 interaction with the backbone atoms, independent of the side chain of these residues. Site directed mutagenesis studies of the rY_1 receptor have suggested that the region around Leu35 in the N-terminal is involved in NPY binding via long range interactions.[19] In the energy minimized average NPY–receptor complex, Leu35 was involved in long range interactions both with Arg19 and Arg25 in NPY, in agreement with the observed decrease in affinity of [^{3}H]-NPY for the Leu35Arg mutant of the rY_1 receptor, compared to the wild type.[19]

Site directed mutagenesis studies have indicated that Trp163, Phe173, Gln219, Asn283 and Phe286 are important for binding of both NPY and BIBP3226.[18]

The present model suggests that the mutation of any of these amino acid residues with alanine would preclude the helical packing, indicating that their role in ligand binding is to maintain the specific packing structure of the TMHs without being directly involved in ligand binding. A rotation of TMH6 such that Asn283 and Phe286 could be directly involved in ligand binding would have precluded the interactions of the ligands with Trp288 and partly with Asp287. A previous molecular modeling study of the Y_1-receptor[30] suggested that Asn283 and Phe286 are involved in ligand interactions, but did not take into account the importance of Trp288[20] for binding of NPY.

In order to become fully activated, the Y_1 receptor needs intact N- and C-terminals.[44] Molecular biology and receptor binding studies have shown that Arg33 and Arg35 of NPY are important for binding to the Y_1 receptor, and that the 1–4 and 31–36 segments of NPY contains a pharmacophore recognized by the Y_1 receptor.[25,26] The design of non-peptidic antagonists for the Y_1 receptor has focused on the structure in the C-terminal region (Arg35 and Tyr36) of NPY,[45] while experimental results indicate that a pharmacophore model for Y_1 receptor activation also should include amino acids in the *N*-terminal region. In the present NPY–receptor complex the Tyr1 hydroxyl oxygen was located 9.2 and 7.3 Å from the terminal nitrogen atoms in the guanidinium group of Arg35. The Tyr1 hydroxyl oxygen - Tyr36 amide nitrogen distance was 7.2 Å, while the Tyr36 amide nitrogen was 7.5 and 6.0 Å from the terminal nitrogen atoms in the guanidinium group of Arg35. The structure of NPY in the energy minimized average structure from 255 to 355 ps of simulation may be considered as the receptor bound conformation of NPY. These interatomic distances may therefore be taken into account in the design of ligands for the Y_1 receptor.

Biochemical studies have indicated that BIBP3226 (Scheme 1) is 10,000 times more potent than its *S*-enantiomer, BIBP3435 in binding to the Y_1 receptor.[45] The calculated binding energies indicated that BIBP3226 has stronger interaction energies with the receptor, mainly due to more favorable interactions between the guanidinium group in BIBP3226 and Asp287 in the receptor, and between the phenyl-rings of the antagonist and aromatic amino acids in the receptor (Table 3).

The binding mode of the PP-family of peptides suggest that the much weaker affinity of PP than of PYY, NPY and [L31, P34]NPY for the hY_1 receptor mainly is a result of the Tyr1Ala and Lys4Glu substitutions in PP (Table 2). These substitutions result in a weaker interaction with the region outside Asp194, Asp200, Gln201, Phe202 in EC loop 2 and Ile293 in EC loop 3 for PP than for the other PP-family peptides (Fig. 4). The binding mode of the peptides also suggested that the main contribution to the weaker affinities of NPY and [L31, P34]NPY than of PYY for the hY_1 receptor was the Ala23Ser substitution in PYY. In the receptor bound conformation of NPY and [L31, P34]NPY, Arg19 had electrostatic interactions with Asp6. However, the Ala23Ser substitution in PYY introduced a hydrogen bond between Asp6 and Ser23, giving Arg19 a possibility for stronger interactions with amino acids in EC loop 3 (Table 2).

Molecular dynamics of receptor activation

The electrostatic potentials of the hY_1 model were mainly negative in the synaptic domains and positive in the cytoplasmic domains (Fig. 2). A similar bipolar distribution of electrostatic charges was also observed in our previous models of the dopamine D_2,[46] serotonin 5-HT_{2A},[47] 5-HT_{1A},[27] 5-HT_{2C}[48] and 5-HT_{1B} receptors.[49] Experimental studies of NPY analogues have shown that the 1–4 and 31–36 segments of NPY contains a pharmacophore recognized by the Y_1 receptor.[25,26] As shown in Fig. 3, both NPY and PP have dipole moments antiparallel to the dipole created by the α-helical structure, producing a highly positive area around the putative receptor binding domains in the N- and C-terminal parts. This charge distribution was also seen for [L31, P34]NPY and PYY, and has previously been demonstrated for NPY and NPY analogues.[50]

The charge distributions suggest that binding of NPY to the hY_1 receptor is initiated by electrostatic interactions between positive domains in NPY and the negative synaptic domains of the hY_1 receptor. These interactions may guide NPY towards its binding site, leading to interactions with key residues in the receptor, most likely optimized by a zipper mechanism,[51] within a cavity formed by the TMHs and the EC parts. The minimized average receptor–NPY and receptor–BIBP3226 complexes provide information about the most populated receptor states in the configurational space that was explored by the simulations. Therefore, based on the R.M.S. differences of TMH5 and TMH6 between the receptor structures from the simulations with NPY and with the antagonist, BIBP3226 (Table 4), we postulate that the main structural differences between the activated receptor and the deactivated receptor are in TMH5 and TMH6 (Fig. 6). The simulations also indicated that NPY introduced larger structural fluctuations in TMH5 and TMH6 than in the other TMHs, while BIBP3226 did not (Table 4). This may indicate that movement of TMH5 and TMH6 relative to other TMHs is important for receptor activation. The packing interactions between TMH5 and TMH6 were similar in the two receptor complexes, indicating that the main contribution to the R.M.S. differences (Table 4) are rigid body motions of the entire TMH5/TMH6 segment. Rigid body motions of TMHs have previously been observed in the light activation of rhodopsin,[52] and rigid body motion of TMH6 has also been suggested to occur in the activation of the muscarine M2 receptor.[53] TMH5 and TMH6 of β_2- adrenergic receptors have been suggested as central in the formation of receptor dimers upon activation.[54] The R.M.S differences of TMH5 and TMH6 between activated and the deactivated receptor states and the larger R.M.S. of fluctuations for TMH5 and TMH6 than for other TMHs during the simulation with NPY, suggest that the interaction of NPY with residues in EC loop 2, and

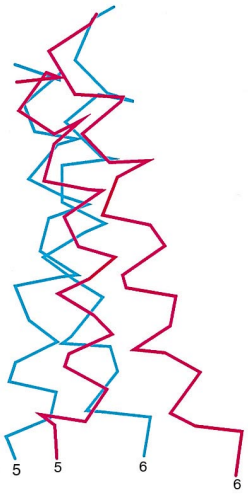

Figure 6. C_α-atom carbon trace of TMH5 and TMH6 of the energy minimized average complex with NPY (blue) and BIBP3226 (red). The figure shows the main structural differences between agonist bound and antagonist bound receptor. The extracellular side is up in the figure. The figure was generated by superimposing TMH1-TMH4 and TMH7 of the two complexes.

with Asp287 and Trp288 at the EC end of TMH6, introduce rigid body motions into the TMH5/TMH6 segment. TMH5 and TMH6 are connected to IC loop 3, which is involved in coupling to G-proteins.[53,55,56] We, therefore, postulate that rigid body motions in TMH5 and TMH6 relative to the other TMHs upon binding of NPY, creates a proper structure of IC loop 3 for G-protein interaction, with the highly positive area outside Arg237, Arg240 and Arg241 exposed to the cytoplasm. The observation that BIBP3226 did not introduce larger fluctuation in TMH5 and TMH6 than in other TMHs suggests that BIBP3226 may function as an antagonist by constraining TMH5 and TMH6 in a position preventing rigid body motions of the TMH5/TMH6 segment relative to the other TMHs, and thus formation of a proper structure of IC loop 3 for G-protein coupling.

Conclusion

Three dimensional models of the hY_1 receptor and its complexes with the peptide ligands NPY, [L31, P34]NPY, PYY, PP, and the small molecule antagonists BIBP3226 and BIBP3435 (*S*-enantiomer of BIBP3226) have been generated. The peptide-receptor complexes suggest that residues 1–4 of the peptides interact with Asp194, Asp200, Gln201, Phe202 and Trp288 in the receptor. Arg33 and Arg35 of the peptides formed salt bridges with Asp104 and Asp287, respectively, while Tyr36 interacted in a binding pocket formed by Phe41, Thr42, Tyr100, Asn297, His298 and Phe302. The electrostatic potentials surrounding the peptide ligands and the hY_1 receptor indicated that ligand binding is initiated by electrostatic interactions between a positively charged region in the N- and C-terminal parts of the peptides, and negatively charged extracellular regions of the receptor. Molecular dynamics simulations of NPY and BIBP3226 in complex with the receptor indicated rigid body motions of TMH5 and TMH6 relative to the other TMHs upon binding of NPY as a mechanism of receptor activation, and that BIBP3226 acts as an antagonist by constraining these motions.

The projection map of visual rhodopsin enables construction of quite reliable models of the TMHs of GPCRs, while structural models of the EC and IC-parts are more uncertain. In the present study, the structural models of loops and terminals were based on secondary structure predictions that give 60–70% correct predictions. The molecular dynamics refinements of loops and terminals, and the flexibility allowed during molecular dynamics simulations of receptor–ligand interactions, may diminish some of the effects of the relatively crude secondary structure predictions. However, these techniques may not overcome all the structural uncertainties inherent in the starting models of loops and terminals. Furthermore, the driving force from lipids and explicit water molecules in generating the preferred side chain geometries is not taken directly into account in the modeling procedure. In spite of the structural constrains based on results from site directed mutagenesis experiments the present ligand–receptor models and the suggested mode of activation, must be considered as rather speculative and need experimental verification.

The helical packing arrangements of TMH1, TMH2, TMH3, TMH5, TMH6 and TMH7 are supported by experimental results. The helical orientation of TMH4 in the model may be validated by site directed mutagenesis studies involving Tyr176. In the present model Tyr176 is packed against Tyr211 at the EC-end of TMH5 and Glu182 in EC2. The model suggest that an alanine mutation of Tyr176 would interfere with the packing of TMH4 against TMH5, and thereby with the BIBP3226 binding site in the region of Tyr211. A further site directed mutagenesis verification of the peptide binding site could involve Phe41, Thr42, Gln201, Phe202 or Asn297, while a verification of the BIBP3226 binding site could involve amino acids included in Table 3.

Methods

Molecular mechanical energy minimization and molecular dynamics simulations were performed with the AMBER 4.0 programs.[57] A distance-dependent dielectric function ($\varepsilon = r_{ij}$), r: interatomic distance) was used in calculations without explicit water molecules. Convergence criterium for molecular mechanical energy minimizations: R.M.S. difference of 0.02 kcal/mol/Å for the norm of the energy gradient between successive steps. Molecular dynamics simulations were performed at 310 K with velocity scaling. The SHAKE option was used to constrain bonds involving hydrogen atoms during the simulation. The step length was 0.001 ps, and the non-bonded pair list was updated after every 10 step during the simulation.

Model building of TMHs

Initial models of the TMHs were constructed from the hY_1 receptor sequence [6] with ϕ and Ψ angles at -57 and $-47°$, respectively. Each TMH was energy refined by 500 cycles of steepest descent minimization followed by 2000 cycles of conjugate gradient minimization. The TMHs were assembled according to the projection map of rhodopsin and a proposed general arrangement of TMHs in GPCRs.[21] The orientations of TMHs relative to each other were based on site directed mutagenesis studies of neuropeptide receptors, using an approach similar to that in a previous model of the rY_1 receptor.[20] Helical kinks were introduced at proline residues in TMH2, TMH5, TMH6 and TMH7. The closely packed TMH bundle was refined by 500 cycles of steepest descent minimization and 2000 cycles of conjugate gradient minimization.

Model building of loops and terminals

Initial models of the loops and terminals were constructed based on secondary structure predictions by the Chou and Fasman method,[58] followed by an energy refinement by 500 cycles of steepest descent minimization and 2000 cycles of conjugate gradient minimization. The EC loops were further refined by 10 cycles of 35 ps simulated annealing molecular dynamics simulation. The loop was gradually heated to 1000 K during the first 5 ps of each cycle, kept at 1000 K between 5 and 15 ps, and gradually cooled to 0 K between 15 and 35 ps. The structure observed after 35 ps of simulation was used as the initial structure in the next cycle of simulated annealing molecular dynamics, which was performed in a similar manner. The structure observed after each cycle was energy minimized until convergence, resulting in 10 different energy minimized structures of each EC loop. The terminal residues were not constrained during the refinement procedure. Potential energy, interactions with the local environments when connected to the TMHs, and the position of key residues for ligand binding were used as criteria for selection among the energy minimized structures.

Model building of the entire hY_1 receptor

The loops and terminals were connected to the TMHs and arranged such that potential interactions with NPY were formed with key residues identified by site directed mutagenesis studies of the hY_1 receptor[16–18] and the rY_1 receptor.[19,20] It has been suggested that a pair of cysteine residues in EC loop 1 and EC loop 2, which are conserved in GPCRs, form a disulphide bond, which, therefore, was introduced between Cys113 and Cys198. The receptor model was refined by 500 cycles of steepest descent energy minimization and 2000 cycles of conjugate gradient minimization, followed by 10 ps of molecular dynamics simulation. The TMHs and residues in the EC parts identified as key residues for binding of NPY (Leu35, Tyr100, Asp104, Asp200, Trp288, His298) were kept at fixed positions during the simulation using the Belly option of the AMBER program. The final coordinate set from the simulation was further refined by 20 ps of molecular dynamics simulation with all the loops and terminals free to move, while the TMHs were kept at fixed positions. The coordinate set obtained after 20 ps of simulation was energy minimized until convergence. The water accessible surface and electrostatic potentials 1.4 Å outside the surface were calculated for the final energy refined model using the MidasPlus program.[59]

Modeling of NPY

The reported structures of NPY in solution are contradictory concerning the C-terminal. A monomeric structure of NPY[4] similar to the crystal structure of avian PP[2] and the NMR structure of bovine PP,[3] while a dimeric structure of NPY[5] suggested that the C-terminal helix extends to Tyr36. From all this, we have chosen to base the initial model of human NPY on the crystal structure of avian PP.[2] A similar approach has also been used by several others to model NPY.[16,30,50] Amino acid residues in PP which are different in PP and NPY, were changed into the corresponding amino acid residues in NPY, such that the position of the backbone atoms were maintained. The initial model was energy minimized and refined by 110 ps of molecular dynamics simulation without any constrains. The structure observed after 110 ps of simulation was energy minimized and used for calculation of the water accessible molecular surface and electrostatic potentials outside the surface, using the MidasPlus program,[59] and for studies of NPY-hY_1 receptor interactions. Models of [L31, P34] and PYY were generated from the NPY model, while a model of human PP was generated from the crystal structure of avian PP. The models of [L31, P34]NPY, PYY and human PP were energy minimized and the water accessible surface and electrostatic potentials outside the surface were calculated. [L31, P34]NPY and PYY are more similar to NPY than avian PP in sequence. Using the NPY model as the initial structure for generating [L31, P34]NPY and PYY, and not avian PP, gave the possibility of a shorter refinement procedure for these peptide structures than for NPY.

Simulation of hY_1 receptor–NPY interactions

NPY was manually docked into the hY_1 receptor model. Guidelines in the docking were: (1) The positions of arginine side chains and terminal tyrosine side chains of NPY. (2) Positions of key residues in the Y_1 receptor for binding of NPY and/or BIBP3226 identified by site directed mutagenesis studies. (3) The water accessible surface and the electrostatic potentials around the surface of NPY and the hY_1 receptor.

The NPY-hY_1 complex was refined by energy minimization until convergence, and used as initial structure in a 355 ps molecular dynamics simulation, with a protocol similar to that used in previous molecular dynamics simulations of GPCRs.[20] Coordinate sets were saved every 1.0 ps during the simulation. The structurally flexible N-terminal of the hY_1 receptor is most probably glycosylated,[6,60] which seem to be a common feature

among GPCRs.[61] To account for the lack of glycosylated N-terminal amino acids in the hY_1 model, a small harmonic force was introduced in order to restrain the structurally flexible N-terminal (residues 1–39) in Cartesian space during the simulation. An average structure was calculated from the coordinate sets observed between 255 and 355 ps of simulation, and energy minimized until convergence.

Ligand–receptor binding energies

The average hY_1-NPY complex between 255 and 355 ps was used as a template for constructing complexes of [L31, P34]NPY, PYY and PP with the hY_1 receptor. The model of PYY, [L31, P34] and PP was superimposed onto the structure of NPY in the energy minimized average complex, and NPY was removed. The ligand–receptor complexes, and the ligand and the receptor structure in each complex, were energy minimized until convergence was obtained. The microscopic binding energies (E_B) of the ligand–receptor complexes were calculated using the following equation:

$$E_B = E_{INT} + E_{LD} + E_{RD}$$

E_{INT}: total interaction energy between the ligand and the receptor. E_{LD}: distortion energy of the ligand, calculated as the difference between the potential energy of the ligand molecule in the energy minimized complex and of the separately energy minimized ligand molecule. E_{RD}: distortion energy of the receptor, calculated as the potential energy difference between the receptor structure in the energy minimized complex and the separately energy minimized receptor structure.

Modeling of BIBP3226

An initial model of BIBP3226 was constructed and energy minimized until convergence with the standard AMBER 4.0 force field. The energy minimized structure of BIBP3226 was used as initial structure in a 150 ps molecular dynamics simulation. Coordinates were saved every 1 ps during the simulation, resulting in 150 different coordinate sets. In order to obtain low-energy conformations of BIBP3226 that might interact with the receptor, each of these coordinate sets were energy minimized until convergence. Clustering analysis of the resulting conformations was not performed.

A similar approach was used to construct a model and span the conformational space of BIBP3435, the S-enantiomer of BIBP3226.

Antagonist-hY_1 receptor interactions

BIBP3226 was originally designed to mimic the C-terminal of NPY,[62] suggesting an overlap between the NPY and BIBP3226 binding sites. Simulation of NPY-hY_1 receptor interactions indicated that Arg33 in NPY forms a salt bridge with Asp104, while Arg35 in NPY forms a salt bridge with Asp287. Site directed mutagenesis studies of BIBP3226-hY_1 receptor interactions have indicated that Asp287 is important for binding of BIBP3226, while Asp104 is not,[18] suggesting that the key residue for interacting with the guanidinium part of BIBP3226 (Scheme 1) is Asp287 at the EC end of TMH6.

BIBP3226 was manually docked into the receptor structure of the energy minimized average receptor-NPY complex from 255 to 355 ps, with the guanidinium part in the direction of Asp287. Several conformations of BIBP3226 were considered and examined manually for their possible molecular interactions with the receptor. The conformation of BIBP3226 giving best structural fit with the receptor model had the guanidinium group close to the hydroxyphenyl-ring. This conformation had about 2 kcal/mol higher energy than the lowest energy conformation of BIBP3226, which enabled interactions between the hydroxyphenyl-group of BIBP3226 and Tyr211 in the receptor. The BIBP3226-hY_1 receptor complex, the receptor model alone and the BIBP3226 structure were energy minimized and the theoretical binding energy was calculated as described for NPY and NPY-analogues.

Several conformations of BIBP3435 were examined for their possibility of interacting with the receptor model. A conformation that enabled interactions between the guanidinium-group of BIBP3435 and Asp287 in the receptor, and the hydroxyphenyl-ring of BIBP3435 and Tyr211 in the receptor, had about 2 kcal/mol higher energy than the lowest energy conformation of BIBP3435. The BIBP3435-receptor complex, the BIBP3435 structure alone and the receptor structure alone were energy minimized and the theoretical binding energy was calculated as previously described.

The energy minimized complex of BIBP3226 with the receptor model was used as starting structure for a 250 ps molecular dynamics simulation of BIBP3226-hY_1 receptor interactions. An average coordinate set for the period between 150 and 250 ps of simulation was calculated and energy minimized until convergence.

References

1. Balasubramaniam, A. *Peptides* **1997**, *18*, 445.
2. Blundell, T. L.; Pitts, J. E.; Tickle, I. J.; Wood, S. P.; Wu, C.-W. *Proc. Natl. Acad. Sci. USA* **1981**, *78*, 4175.
3. Li, X.; Sutcliffe, M. J.; Schwartz, T. W.; Dobson, C. M. *Biochemistry* **1992**, *31*, 1245.
4. Darbon, H.; Bernassau, J. M.; Deleuze, C.; Chenu, J.; Roussel, A.; Camillau, C. *Eur. J. Biochem.* **1992**, *209*, 765.
5. Cowley, D. J.; Hoflack, J. M.; Pelton, J. T.; Saudek, V. *Eur. J. Biochem.* **1992**, *205*, 1099.
6. Herzog, H.; Hort, H. J.; Ball, H. J.; Hayes, G.; Shine, J.; Selbie, L. A. *Proc. Natl. Acad. Sci. USA* **1992**, *89*, 5794.
7. Larhammar, D.; Blomqvist, A. G.; Yee, F.; Jazin, E.; Yoo, H.; Wahlested, C. *J. Biol. Chem.* **1992**, *267*, 10935.
8. Krause, J.; Eva, C.; Seeburg, P. H.; Sprengel, R. *Mol. Pharmacol.* **1992**, *41*, 817.
9. Rose, P. M.; Fernandes, P.; Lynch, J. S.; Frazier, S. T.; Fisher, S. M.; Kodukula, K.; Kienzle, B.; Seethala, R. *J. Biol. Chem.* **1995**, *270*, 22661.
10. Bard, J. A.; Walker, M. W.; Branchek, T. A.; Weinshank, R. L. *J. Biol. Chem.* **1995**, *270*, 26762.

11. Lundell, I.; Blomqvist, A. G.; Berglund, M. M.; Schober, D. A.; Johnson, D.; Statnick, M. A.; Gadski, R. A.; Gehlert, D. R.; Larhammar, D. *J. Biol. Chem.* **1995**, *270*, 29123.
12. Weinberg, D. H.; Sirinathsinghji, D. J.; Tan, C. P.; Shiao, L. L.; Morin, N.; Rigby, M. R.; Heavens, R. H.; Rapoport, D. R.; Bayne, M. L.; Cascieri, M. A.; Strader, C. D.; Linemeyer, D. L.; MacNeil, D. J. *J. Biol. Chem.* **1996**, *271*, 16435.
13. Gerald, C.; Walker, M. W.; Criscione, L.; Gustafson, E. L.; Batzl-Hartmann, C.; Smith, K. E.; Vaysse, P.; Durkin, M. M.; Laz, T. M.; Linemeyer, D. L.; Schaffhauser, A. O.; Whitebread, S.; Hofbauer, K. G.; Taber, R. I.; Branchenk, T. A.; Weinshank, A. *Nature* **1996**, *382*, 168.
14. Pebay-Peyroula, E.; Rummel, G.; Rosenbusch, J. P.; Landau, E. M. *Science* **1997**, *277*, 1676.
15. Unger, V. M.; Hargrave, P. A.; Baldwin, J. M.; Schertler, G. F. X. *Nature* **1997**, *389*, 203.
16. Walker, P.; Munoz, M.; Martinez, R.; Peitsch, M. *J. Biol. Chem.* **1994**, *269*, 2863.
17. Sautel, M.; Martinez, R.; Munoz, M.; Peitsch, M. C.; Beck-Sickinger, A. G.; Walker, P. *Mol. Cell. Endocrinol.* **1995**, *112*, 215.
18. Sautel, M.; Rudolf, K.; Wittneben, H.; Herzog, H.; Martinez, R.; Munoz, M.; Eberlein, W.; Engel, W.; Walker, P.; Beck-Sickinger, A. G. *Mol. Pharmacol.* **1996**, *50*, 285.
19. Robin-Jagerschmidt, C.; Sylte, I.; Bihoreau, C.; Hendricksen, L.; Calvet, A.; Dahl, S. G.; Bénicourt, C. *Mol. Cell. Endocrinol.* **1998**, *139*, 187.
20. Sylte, I.; Robin-Jagerschmidt, C.; Bihoreau, C.; Hendricksen, L.; Calvet, A.; Bénicourt, C.; Dahl, S. G. *J. Mol. Model.* **1998**, *4*, 221.
21. Baldwin, J. M. *EMBO J.* **1993**, *12*, 1693.
22. Nicholls, A.; Honing, B. *J. Comput. Chem.* **1991**, *40*, 3254.
23. Kirby, D. A.; Boublik, J. H.; Rivier, J. E. *J. Med. Chem.* **1993**, *36*, 3802.
24. Kirby, D. A.; Koerber, S. C.; Craig, A. G.; Feinstein, R. D.; Delmas, L.; Brown, M. R.; Rivier, J. E. *J. Med. Chem.* **1993**, *36*, 385.
25. Beck-Sickinger, A. G.; Wieland, H. A.; Wittneben, H.; Willim, K.-D.; Rudolf, K.; Jung, G. *Eur. J. Biochem.* **1994**, *225*, 947.
26. Fournier, A.; Gagnon, D.; Quirion, R.; Dumont, Y.; Pheng, L.-H.; St-Pierre, S. *Mol. Pharmacol.* **1994**, *45*, 93.
27. Sylte, I.; Edvardsen, Ø.; Dahl, S. G. *Protein Eng.* **1996**, *9*, 149.
28. Sylte, I.; Chilmonczyk, Z.; Dahl, S. G.; Cybulski, J.; Edvardsen, Ø. *J. Pharm. Pharmacol.* **1997**, *49*, 698.
29. Paterlini, G.; Portoghese, P. S.; Ferguson, D. M. *J. Med. Chem.* **1997**, *40*, 3254.
30. Du, P.; Salon, J. A.; Tamm, J. A.; Hou, C.; Cui, W.; Walker, M. W.; Adham, N.; Dhanoa, D. S.; Islam, I.; Vaysse, P. J.-J.; Dowling, B.; Shifman, Y.; Boyle, N.; Rueger, H.; Schmidlin, T.; Yamaguchi, T.; Branchek, T. A.; Weinshank, R. L.; Gluchowski, C. G. *Protein Eng.* **1997**, *10*, 109.
31. Zhou, W.; Flanagan, C.; Ballesteros, J. A.; Konvicka, K.; Davidson, J. S.; Weinstein, H.; Millar, R. P.; Sealfon, S. C. *Mol. Pharmacol.* **1994**, *45*, 165.
32. Sealfon, S. C.; Chi, L.; Ebersole, B. J.; Rodie, V.; Zhang, D.; Ballesteros, J. A.; Weinstein, H. *J. Biol. Chem.* **1995**, *270*, 16683.
33. Perlman, J. H.; Colson, A.-O.; Wang, W.; Bence, K.; Osman, R.; Gerengorn, M. C. *J. Biol. Chem.* **1997**, *272*, 11937.
34. Barak, L. S.; Menard, L.; Ferguson, S. S. G.; Colapietro, A.-M.; Caron, M. G. *Biochemistry* **1995**, *34*, 15407.
35. Liu, J.; Schoneberg, T.; van Rhee, M.; Wess, J. *J. Biol. Chem.* **1995**, *270*, 19532.
36. Groblewski, T.; Maigret, B.; Larguier, R.; Lombard, C.; Bonnafous, J.-C. *J. Biol. Chem.* **1997**, *272*, 1822.
37. Balmforth, A. J.; Lee, A. J.; Warburton, P.; Donnelly, D.; Ball, S. G. *J. Biol. Chem.* **1997**, *272*, 4245.
38. Mizobe, T.; Maze, M.; Lam, V.; Suryanarayana, S.; Kobilka, B. K. *J. Biol. Chem.* **1996**, *271*, 2387.
39. Rao, V. R.; Cohen, G. B.; Oprian, D. D. *Nature* **1994**, *367*, 639.
40. Elling, C. E.; Møller Nielsen, S.; Schwartz, T. W. *Nature* **1995**, *374*, 74.
41. Elling, C. E.; Schwartz, T. W. *EMBO J.* **1996**, *15*, 6213.
42. Thirstrup, K.; Elling, C. E.; Hjort, S. A.; Schwartz, T. W. *J. Biol. Chem.* **1996**, *271*, 7875.
43. Cappelli, A.; Anzini, M.; Vomero, S.; Menziani, M. C.; Benedetti, P. G.; Sbacchi, M.; Clarke, G. D.; Mennuni, L. *J. Med. Chem.* **1996**, *39*, 860.
44. Grundemar, L.; Håkanson, R. *Gen. Pharmac.* **1993**, *24*, 785.
45. Lundberg, J. M.; Modin, A.; Malmstrøm, R. E. *T.I.P.S.* **1996**, *17*, 301.
46. Dahl, S. G.; Edvardsen, Ø.; Sylte, I. *Proc. Natl. Acad. Sci. USA* **1991**, *88*, 8111.
47. Edvardsen, Ø.; Sylte, I.; Dahl, S. G. *Brain Res. Mol. Brain Res.* **1992**, *14*, 166.
48. Kristiansen, K.; Dahl, S. G. *Eur. J. Pharmacol.* **1996**, *306*, 195.
49. Kristiansen, K.; Edvardsen, Ø; Dahl, S. G. *Receptors and Channels* **1998**, *6*, 31.
50. Bjørnholm, B.; Jørgensen, F. S.; Schwartz, T. W. *Biochemistry* **1993**, *32*, 2954.
51. Burgen, A. S. V.; Roberts, G. C. K.; Feeney, J. *Nature* **1975**, *253*, 753.
52. Farrens, D. L.; Altenbach, C.; Yang, K.; Hubbell, W. L.; Khorana, H. G. *Science* **1996**, *274*, 768.
53. Liu, J.; Blin, N.; Conklin, B. R.; Wess, J. *J. Biol. Chem.* **1996**, *271*, 6172.
54. Gouldson, P. R.; Snell, C. R.; Bywater, R. P.; Higgs, C.; Reynolds, C. A. *Protein Eng.* **1998**, *11*, 1181.
55. Eason, M. G.; Ligget, S. B. *J. Biol. Chem.* **1995**, *270*, 24753.
56. Damaj, B. B.; McColl, S. R.; Neote, K.; Songqing, N.; Ogborn, K. T.; Hebert, C. A.; Naccache, P. H. *FASEB J.* **1996**, *10*, 1426.
57. Weiner, S. J.; Kollman, P. A.; Case, D. A.; Singh, U. C.; Ghio, C.; Alagona, G.; Profeta, Jr., S.; Weiner, P. *J. Am. Chem. Soc.* **1984**, *106*, 765.
58. Chou, P. Y.; Fasman, G. D. *Annu. Rev. Biochem.* **1978**, *47*, 251.
59. Ferrin, T. E.; Huang, C. C.; Jarvis, L. E.; Langridge, R. *J Mol. Graphics* **1988**, *6*, 1.
60. Sheikh, S. P.; Roach, E.; Fuhlendorff, J.; Williams, J. A. *Am. J. Physiol.* **1991**, *260*, G250.
61. Dohlman, H. G.; Thorner, J.; Caron, M. G.; Lefkowitz, R. *J. Annu. Rev. Biochem.* **1991**, *60*, 653.
62. Rudolf, K.; Eberlein, W.; Engel, W.; Wieland, H. A.; Willim, K. D.; Entzeroth, M.; Wienen, W.; Beck-Sickinger, A. G.; Doods, H. N. *Eur. J. Pharmacol. Mol. Pharm. Sect.* **1994**, *271*, R11.